Na_2IrO_3 as a molecular orbital crystal

I. I. Mazin[1], H. O. Jeschke[2], R. Valentí[2], and D. I. Khomskii[3]
[1] *Code 6393, Naval Research Laboratory, Washington, DC 20375, USA*
[2] *Institut für Theoretische Physik, Goethe-Universität Frankfurt am Main, 60438 Frankfurt am Main, Germany and*
[3] *II. Physikalisches Institut, Universität zu Köln, Zülpicher Strasse 77, 50937 Köln, Germany*
(Dated: May 17, 2012)

Spin-orbit (SO) coupling can lead to many nontrivial effects in such fields as spintronics (Rashba effect), topological insulators, or to the formation of topologically protected states in systems described by the Heisenberg-Kitaev model, recently proposed for Na_2IrO_3. This proposal is based on the fact the SO coupling for Ir is very strong. We show, however, that Na_2IrO_3 represents a highly unusual case, in which the electronic structure is dominated by the formation of quasi-molecular composite orbitals (QMOs). The QMOs consist of six atomic orbitals on an Ir hexagon, and the orbital moment of each QMO is quenched. The concept of such QMOs in solids is completely new, and invokes very different physics compared to the models considered previously. For instance, one has to account for Hubbard correlations among the QMOs, and not individual atomic orbitals. Both, the insulating behavior and the experimentally observed zigzag antiferromagnetism in Na_2IrO_3 naturally follow from the QMO model.

PACS numbers: 75.10.-b,75.10.Jm,71.70.Ej,71.15.Mb

The recent discovery of quasihexagonal sodium iridate Na_2IrO_3, see *e.g.* Ref. 1 with a honeycomb lattice of Ir^{4+} ($5d^5$) ions has generated enormous interest. A very nontrivial hierarchy of energy scales, with spin-orbit coupling exceeding the three energies typically dominating the physics of $3d$ and $4d$ transition metals (the Hubbard U, the Hund's J_H, and the one-electron hopping t), has been proposed theoretically [2], and shown to have a highly nontrivial phase diagram[2, 3]. It is presumed in this so-called Heisenberg-Kitaev model that the three orbitals forming the t_{2g} band of Ir d states are nearly degenerate in energy and their hopping between sites is limited by the nearest neighbor (n.n.) bonds and proceeds through two main channels. One is the direct overlap of the Ir d orbitals, t_1, and the other an assisted hopping through oxygen p orbitals, $t_1' = t_{pd\pi}^2/(E_F - E_p)$, where E_F is the Fermi energy lying in the d band, *i.e.* $E_F \sim E_d$. For ideal IrO_6 octahedra this latter hopping is allowed, for each of the three n.n. bonds, only between a particular pair of unlike orbitals, for instance, between d_{xz} and d_{yz}. It is further assumed that the spin-orbit interaction is much larger than any one-electron hopping. If that were the case, the degeneracy of the t_{2g} orbitals would have been lifted and the ground state would be a Kramers doublet with total angular momentum (effective spin) 1/2. From the one-electron point of view, this means that the three real harmonics do not represent a good basis to describe the t_{2g} states; a better basis would be one that maximizes the angular moment [4, 5]: $d_{xz} + id_{yz}$, $d_{yz} + id_{xy}$, and $d_{xy} + id_{xz}$. A strong spin-orbit will hold the spins of these complex orbitals parallel to z, y, and x, respectively. If only hopping *via* oxygen p orbitals is allowed (see a detailed discussion later in this paper), and the Ir-O-Ir angles are all 90^o, then for each of these complex orbitals there will be one particular bond direction where the effective hopping will be maximized. According to the Goodenough-Kanamori rules, in this case the magnetic coupling along this bond will be ferromagnetic, and maximized when the spins are parallel to the corresponding (different for each bond) quantization axis, with the coupling strength of the order of $J_O t_{pd\pi}^4/(E_F - E_p)^4 = J_O[t_1'/(E_F - E_p)]^2$, where J_O is the Hund's rule coupling on oxygen. Combined with the direct Heisenberg exchange of the order of t_1^2/U, these considerations lead to the following Hamiltonian, usually called "Heisenberg-Kitaev" [2]:

$$H_{ij} = J_{\rm A}\mathbf{S}_i \cdot \mathbf{S}_j - J_{\rm F} S_i^\gamma S_j^\gamma, \qquad (1)$$

where S_i is the effective spin formed at site i. For each pair i, j there exists one particular cubic direction $\gamma = x, y$ or z. Here $J_{\rm A} > 0$ is the Heisenberg antiferromagnetic term and $J_{\rm F} > 0$ is the ferromagnetic superexchange[8]. This Hamiltonian leads to a nontrivial phase diagram, including a quantum spin liquid phase with gapless excitations of Majorana fermion type at large $J_{\rm F}$ [6]. Recently, a modification of this model with considerable 2nd and 3rd n.n. Heisenberg exchange interactions has also been proposed [7] mainly because the original model failed to describe the existing experimental data.

This model (Eq. (1)), however, implies a very particular hierarchy of energies, namely the spin-orbit interaction must dominate over both the one-electron hopping and the trigonal crystal field splitting of the t_{2g} orbitals. Also, in order to ensure a long range magnetic order in this model the superexchange interaction should be comparable with the direct exchange.

It appears that both these conditions are violated in Na_2IrO_3. It has been pointed out [9] that the real, accurately determined crystal structure of Na_2IrO_3 [9, 10] features Ir-O-Ir bond angles that are close to 98^o. Note that for $5d$ metals $U \sim 1 - 1.5$eV $\ll (E_F - E_p)$. In this regime the ferromagnetic part of the superexchange is

determined by the ratio $J_O[t_1'/(E_F - E_p)]^2$, while the antiferromagnetic part by the ratio $(t_1')^2/U$. Given that $J_O \sim U \ll (E_F - E_p)$, it becomes obvious that the net interaction is only ferromagnetic in a narrow range of angles close to 90^o, where the antiferromagnetic superexchange disappears [11]. An angle of 98° is clearly outside this range.

Secondly, the total width, W, of the t_{2g} band is about 1.5 eV, which is larger than the spin-orbit coupling $\lambda \lesssim 0.5$ eV thus violating the first condition of the Heisenberg-Kitaev model as well.

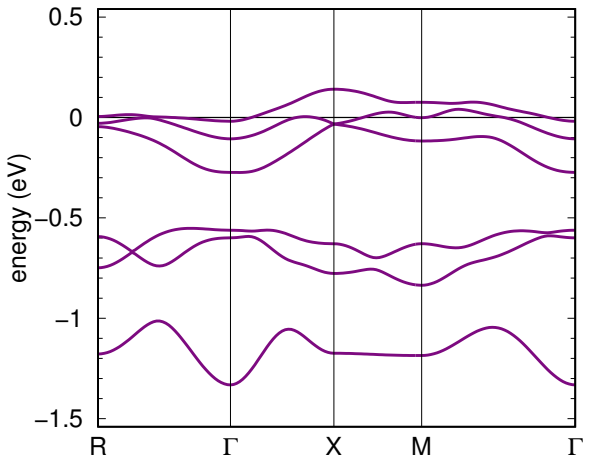

FIG. 1: (a) Electronic structure for the non-magnetic state of Na_2IrO_3 without inclusion of spin-orbit coupling for the experimentally determined crystal structure. The calculations were performed with the full potential local orbital (FPLO) basis using the generalized gradient approximation (see Suppl. Information).

Note that the spin-orbit coupling λ is largely reduced by hybridization with oxygen and, as explained below, by the quenching of the orbital moment. The trigonal splitting Δ_T could be in principle large, but appears small because of cancellation of various factors, as shown below.

How then should one approach the electronic structure of this compound, given that the energy hierarchy is in reality $W > U > \lambda > J_H > \Delta_T$?

In order to answer this question, we have first performed *ab initio* calculations [12] of the electronic structure, using the experimentally determined $C\,2/m$ structure [9], without including the spin-orbit coupling (Fig. 1). A cursory glance at the calculated band structure reveals a picture rather removed from the naive quasiatomic considerations underlying Eq. (1): instead of the expected splitting of the 6 t_{2g} states (there are two Ir atoms per unit cell) into two a_{1g} and four e_g' states, we observe an ordering of the states into a single-state band at ~ -1.2 eV, a two-states one at ~ -0.6 eV, and a three-states manifold at the Fermi level, which, as we shall see later, consists of slightly overlapping two-states and single-state bands.

TABLE I: Six quasi-molecular orbitals formed by the six t_{2g} atomic orbitals on a hexagon. Here $\omega = \exp(i\pi/3) = \frac{1}{2} + i\frac{\sqrt{3}}{2}$, $\omega^2 = \exp(2i\pi/3) = -\frac{1}{2} + i\frac{\sqrt{3}}{2} = -\omega^*$, $\omega^3 = -1$, $\omega^4 = \exp(4i\pi/3) = -\frac{1}{2} - i\frac{\sqrt{3}}{2} = -\omega$, $\omega^5 = \exp(5i\pi/3) = \frac{1}{2} - i\frac{\sqrt{3}}{2} = \omega^*$, $\omega^6 = 1$

Symmetry	Eigenenergy	Eigenvector(s)
A_{1g}	$-2t_1'$	1,1,1,1,1,1
E_{1u}	$-t_1'$	1, ω, ω^2, −1, ω^4, ω^5
(twofold)		1, ω^5, ω^4, −1, ω^2, ω
E_{2g}	t_1'	1, ω^2, ω^4, 1, ω^2, ω^4
(twofold)		1, ω^4, ω^2, 1, ω^4, ω^2
B_{1u}	$2t_1'$	1,-1,1,-1,1,-1

To analyze this band structure, we have inverted it using the Wannier function formalism (see Suppl. Information), and extracted the hopping parameters up to the 3rd neighbors. We have found that by far the largest single parameter is the O-assisted n.n. hopping, t_1' =262±2 meV. Therefore, a sensible starting point is the electronic structure obtained by retaining only t_1' and setting all other parameters to zero.

Let us first look at the crystal structure of Na_2IrO_3 in a cubic setting, as shown in Fig. 2(a). The three types of Ir-Ir bonds are parallel to the cubic directions (110), (101), and (011). We call them, respectively, xy, xz and yz bonds. As illustrated in Fig. 2(b), the only allowed Ir-O $pd\pi$ hopping path along, for instance, the xy bond (blue lines) takes us from the d_{xz} orbital of one Ir to the d_{yz} one of a neighboring Ir, and so on. Let us now consider an individual orbital, say, d_{xy}, on a site that in Fig. 3 is labeled as "1". An electron can only hop along the yz (red line) bond, into the d_{xz} state on site 2, or along the xz (green line) bond, into the d_{yz} state on site 6. Following the allowed hoppings we realize that an electron starting in a particular orbital state will be always localized on one hexagon, as there are no hoppings in the system that would mix the states on two hexagons. The quasi-molecular composite orbital so formed can be written down as a linear combination of the 6 states on a particular hexagon; the problem is mathematically similar to the molecular π-orbitals of benzene, or to the hypothetical SH_6 molecule considered in the text book [13], except that here the quasi-molecular orbital is formed by three alternating atomic orbitals. As discussed in Ref. [13], the exact solution for the possible phase combinations of the component orbitals yields four eigenstates as shown in Table 1.

Thus, we have a new basis for constructing our wave functions: instead of two sites per cell, with the total of 6 atomic t_{2g} orbitals, we have one hexagon per cell (which

FIG. 2: (a) Crystal structure of Na_2IrO_3 in the cubic setting. The hexagonal direction is along the 111 direction in this setting. Ir, O and Na atoms are shown as grey, magenta, and yellow spheres, respectively. The three inequivalent Ir-Ir bonds are labeled according to their cubic directions. (b) A cartoon illustrating formation of a quasi-molecular orbital on an Ir_6 hexagon. If only hopping *via* O p states is allowed, for each of the three Ir-Ir bond types only hopping between two particular t_{2g} orbitals is possible. The same holds for the second and third nearest neighbor hopping *via* O p and Na s orbitals. Ir-Ir bonds are color coded as follows: xy bonds are shown by blue lines, xz bonds by green, and yz bonds by red ones.

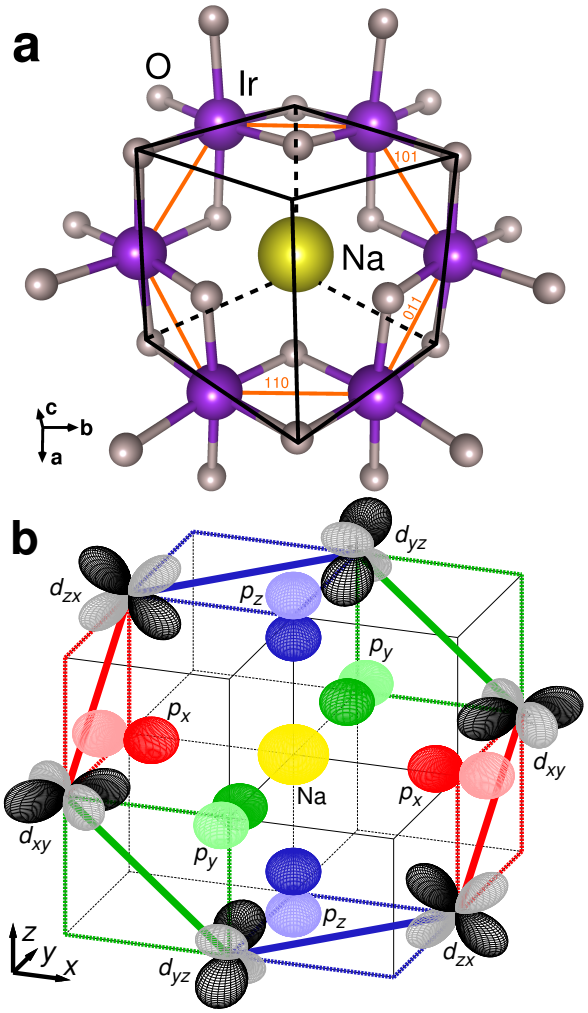

can be identified by the Na atom in the center), with 6 composite orbitals per "site" (hexagon).

The next most important hoppings are second n.n. ones between unlike orbitals, which proceed *via* the two closest oxygen p orbitals and the diffuse Na s orbital. These become particularly important if the O octahedra around Ir are trigonally squeezed (as they are). According to our calculation, these hoppings are 79-80 meV,

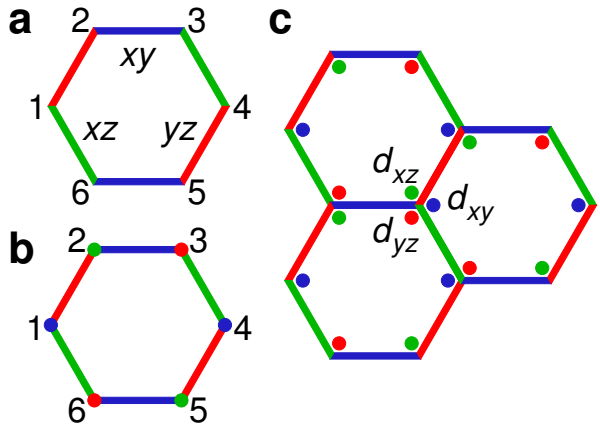

FIG. 3: (a) Schematic plot of a Ir_6Na hexagon. We use the same color coding as in Fig. 2, xy bonds are shown by blue lines and d_{xy} orbitals by blue dots, *etc.* (b) A quasi-molecular composite orbital on a given hexagon. (c) Three neighboring quasi-molecular orbitals.

3.3 times smaller than t_1'. To the lowest order their amplitude is given by $t_2' \sim t_{pd\pi}^2 t_{sp}^2/(E_F - E_p)^2(E_s - E_F)$, where the index s refers to Na s orbital. Importantly, these hoppings take us from the d_{xy} orbital on site 1 to the d_{yz} orbital on site 3, *etc.*, again leaving the electron within the same composite orbital. All other hoppings, including the direct $dd\sigma$ overlap implied in Eq. (1), are at least a factor of two smaller. [14]

It is interesting that the trigonal splitting Δ, which also couples the n.n. QMOs, is small (< 25 meV) even though the distortion itself is large. This can be understood from the fact that three factors of comparable magnitude determine the value of Δ [15]: the ratio between the iridium-oxygen $t_{pp\sigma}/t_{pp\pi}$ (the sign of the ligand field depends on this ratio), the electrostatic field on the Ir site, and the fact that the a_{1g} orbital extends over towards the positively charged Na (see Suppl. Information), and is thus pushed down compared to the e_2' orbitals. Apparently in the actual crystal structure of Na_2IrO_3 these three factors largely cancel out.

Looking at the actual *non-relativistic* bands of Na_2IrO_3, we see that the overall structure deduced in the previous paragraphs survives (Fig. 1). The lowest band is singly degenerate and separated from the next one. The next lowest band is doubly degenerate, as expected. However, the two upper bands (E_{2g} and B_{1u}) slightly overlap. At the energy where they overlap a peak in the DOS appears (Fig. 4) because of flat band dispersion in that energy range. This peak has interesting consequences. In the same figure we show the calculated non-relativistic DOS in the ferromagnetic state. Since the non-magnetic Fermi level appears close to this peak, the system is unstable against ferromagnetism and exchange splitting of the peak. The high DOS drives the system into the half-metallic state where the majority bands are

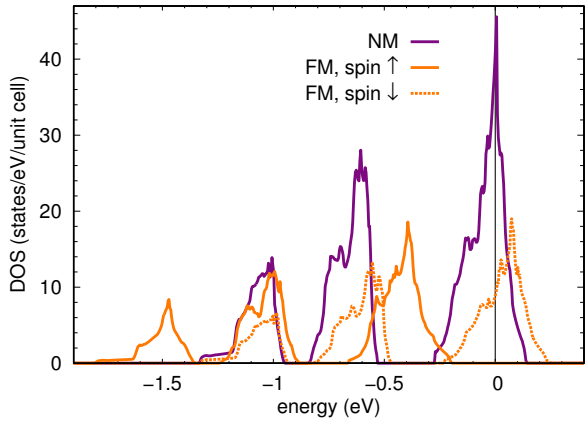

FIG. 4: Non-magnetic (purple) and ferromagnetic (orange) density of states (DOS) of Na_2IrO_3 calculated with the FPLO basis using the generalized gradient approximation without spin-orbit coupling (see Suppl. Information).

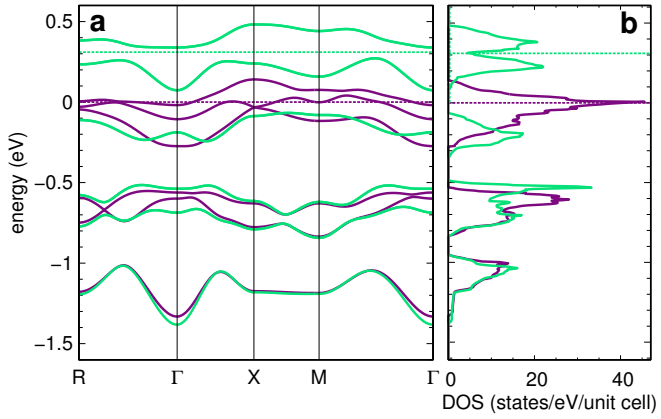

FIG. 5: Effect of spin-orbit on the band structure (a) and DOS (b) of Na_2IrO_3. The purple and green lines refer to the non-magnetic calculation without and with spin-orbit interaction, respectively. Note that the Fermi levels (shown by the horizontal dashed lines) are not aligned.

fully occupied and the Fermi level cuts the minority band right in the middle of the E_{2g} band. Obviously, this is a rather fragile situation, related to a particularly high DOS at the Fermi level in the non-relativistic calculations, and one may expect the spin-orbit interaction to change the magnetic ground state significantly just by modifying the DOS.

Now that we have established the mechanism of formation of the *non-relativistic* band structure, let us see how turning on the spin-orbit coupling affects it. Here another surprise awaits us. As Fig. 5 shows, the effect is rather moderate. It is obvious that the spin-orbit interaction is strong but not dominant. Moreover, the lower two manifolds, well isolated, experience only a very minor spin-orbital effect, not more than 50 meV, and only a few meV on average. The upper subbands, as mentioned previously, overlap and mix, which leads to sizable changes, from 0.2 to 0.5 eV. Interestingly, the overlapped manifold of two E_{2g} and one B_{1u} bands has now essentially split into three individual subbands (which one cannot any longer, strictly speaking, call E_{2g} and B_{1u}, but the notion of the QMOs involving 6 atomic orbitals each still holds). Now it becomes virtually impossible to produce a half-metallic $S = 1/2$ state, as in the non-relativistic case: an exchange splitting of ~ 0.5 eV, corresponding to $M = 1\ \mu_B$, is smaller than the combined band width of the upper two bands.

All these seemingly unexpected results are in fact natural consequences of the QMO picture. Indeed, let us consider first the A_{1g} band (see Table I), and limit ourselves to the t_1' only model (dispersionless bands). This QMO has the same phases on all 6 sites. Let us consider the spin-orbit interaction $\hat{\mathbf{L}}\cdot\hat{\mathbf{S}}$ at a given $\mathbf{k}$-point, between two QMOs. Let us say, to be specific, that they share an "xy" bond, between the sites "2" and "3" in Fig. 3. Let us further say that the distance between the centers of the two QMOs is $\mathbf{R}$, so that the phase factor between the two QMOs is $\exp(i\mathbf{kR})$. The two orbitals on sites 2 and 3 are d_{xz} and d_{yz} (the first QMO) and d_{yz} and d_{xz} (the second QMO), respectively. The matrix elements of the orbital moment operator $\hat{\mathbf{L}}$ on site 2 and 3 is then

$$\mathbf{L}_2 = \mathbf{L}_3^* = \left\langle d_{xz} + \exp(i\mathbf{kR})d_{yz}|\hat{\mathbf{L}}|d_{xz} + \exp(-i\mathbf{kR})d_{yz}\right\rangle . \quad (2)$$

Since there is another QMO, located at $-\mathbf{R}$, and involving the same atomic orbitals on sites 5 and 6, the corresponding matrix elements also need to be added.

A direct calculation shows that $\mathbf{L}_2 \neq 0$, $\mathbf{L}_2 = \mathbf{L}_3 = -\mathbf{L}_5 = -\mathbf{L}_6$, and their contributions cancel identically. A bit more tedious arithmetic shows that the two-fold E_{1u} state also has zero matrix elements of the angular momentum, both diagonal and off-diagonal.

This is not the case for the matrix elements between the B_{1u} and any of the E_{2g} states, forming the three upper bands. Acting the same way, one can show that the sum of all four components is nonzero, and, indeed, in the calculations these states are strongly affected by the spin-orbit coupling. As a consequence, the manifold of the three bands splits into three individual bands; their dispersion also increases. This broadening of the upper bands is the factor preventing the system from getting fully spin-polarized in the ferromagnetic calculations, and reducing substantially the energy gain in the magnetic state.

Importantly, as a result of the hybridization between the E_{2g} and the B_{1u} bands, the latter becomes fully separated with only a tiny indirect overlap. [16] Since a gap or pseudogap at the Fermi level is advantageous from the point of view of the one-electron energy, one can expect that such a non-magnetic band structure should promote magnetic patterns that do not destroy the pseudogap. As

we shall see, the stripy pattern (and, of course, the ferromagnetic one) destroy the pseudogap, but the zigzag pattern preserves it (see Fig. 6). This gives the latter a serious energetic advantage.

Let us now discuss the possibility of a Mott-Hubbard state in this system. In previous works sometimes values of U of 3 eV and larger were considered [17, 18]. This is an unjustifiably large number, appropriate for $4d$, but not $5d$ metals. Generally speaking, U is reduced by about 1 eV when going to $4d$ metals (a typical value being 2-3 eV) and by about as much when moving to the fifth period. A quasiatomic estimate of U and J in Na_2IrO_3 using the recipe from Ref. [19], yields $U = 1.68$ eV and $J = 0.29$ eV. With these values, $U - J$ is not enough to drive the whole t_{1g} band into a Mott regime, because its width W is larger than U. On the other hand, the individual subbands are much narrower, and can be strongly correlated in the Mott-Hubbard sense. In this case, however, the relevant energy is not the atomic U, but U_{QMO}, the energy cost of placing an extra electron on a QMO. This is similar to correlation effects in the narrow t_{1u} band in fullerides [20]. Of course, U_{QMO} is much smaller than U; assuming no additional screening by other QMOs, $U_{QMO} \sim U/6 \lesssim 0.3$ eV. While this seems like a small number, it is to be compared to the band width of the individual subbands, which for the top three bands is also 0.2-0.3 eV. This situation is very similar to the Mott state in TaS_2, where the CDW combined with the spin-orbit interaction creates an isolated very narrow band, which experiences a Mott transition even though U is only a small fraction of an eV.

The U_{QMO}, in the non-magnetic state, can enhance the already existing, but extremely small gap in the fully relativistic DFT calculations (the minimal indirect gap is zero within the computational accuracy, while the average direct, *i.e.*, optical gap is about 150 meV), however it would be probably misleading to call the material a Mott insulator, since it is already nonmetallic in DFT when including spin-orbit coupling. This fact has been recently also pointed out in Ref. 18.

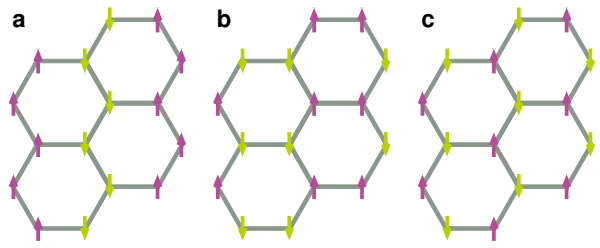

FIG. 6: Three antiferromagnetic patterns considered in this paper: (a) zigzag, (b) stripy, and (c) Néel.

It has been common to try to describe the magnetic ground state in terms of n.n. (up to 3rd neighbors) exchange of various kinds [7]. Given enough parameters, any given state can be reproduced. In this capacity, mapping effective interactions onto an effective Heisenberg model has been successfully applied to materials where electrons are not localized at all and the concept of superexchange is not applicable (metal Fe, or Fe-based superconductors, for instance). We shall adopt however a different approach and try to speculate about possible magnetic orderings in terms of QMOs, which, as we have established, play a crucial role in the electronic structure of Na_2IrO_3. Since the non-magnetic ground state is insulating, and the magnetic moment is small, one naturally expects an antiferromagnetic ordering. To find out which orders are naturally compatible with the QMO picture, let us consider possible antiferromagnetic patterns and simply calculate the energy of the highest (unoccupied) QMO for a given pattern. On the one-electron energy level, the pattern where the highest level has the largest energy will win (because its occupied QMOs, combined, will have the lowest energy).

The Hamiltonian we need to diagonalize is

$$\Delta_{ex} s_i \delta_{ij} + t\delta_{i+1,j} \tag{3}$$

where $i = \{1...6\}$, and s_i takes $+1$ or -1, depending on the pattern (Fig. 6). Δ_{ex} is the exchange splitting. Specifically, in the Néel state $s_i = \{+1,-1,+1,-1,+1,-1\}$, in the stripy phase $s_i = \{\pm 1, \mp 1, \mp 1, \pm 1, \mp 1, \mp 1\}$, where half of the hexagons assume the upper sign, and half the lower, and in the zigzag phase $s_i = \{+1,+1,+1,-1,-1,-1\}$. Diagonalizing the Hamiltonian, we find the energy of the upper orbital to be, respectively, $\sqrt{4t^2+\Delta_{ex}^2}$, $t/2 + \sqrt{9t^2+4t\Delta_{ex}+4\Delta_{ex}^2}/4 + \sqrt{9t^2-4t\Delta_{ex}+4\Delta_{ex}^2}/4$ (after the averaging over both types of hexagons) and $\sqrt{5t^2/2+\Delta_{ex}^2 + t\sqrt{9t^2/4+8\Delta_{ex}^2}}$. The ferromagnetic state in this model has no energy gain if $\Delta_{ex} \le t/2$, and $t-2\Delta_{ex}$ otherwise. An elementary calculation shows that the zigzag configuration is always the lowest among antiferromagnetic states (Fig. 7). Ferromagnetism is competitive with the zigzag patter, the actual winner being defined by a fine balance between the Hund's J and the one-electron energy scales t and SO. Indeed in the DFT calculations the energies of these two states are very close. Such frustration, combined with high itinerancy inside the hexagons, suggests that the magnetic long range order (T_N) and the spin response (Curie-Weiss temperature Θ_{CW} in susceptibility) may be decoupled in this system, and indeed the measured Θ_{CW} is much larger than T_N.

This picture is, strictly speaking, applicable for the fully isolated QMO model, which, as we know, is a good approximation for the three lower bands, A_{1g} and E_{2u}, but not as good for the upper three, E_{2g} and B_{1u}. Indeed in the DFT calculations without spin-orbit the order of the magnetic states differs: the ground state is ferromagnetic, the Néel state is (as in the model) the least stable, but the zigzag and the stripy phase come out essentially

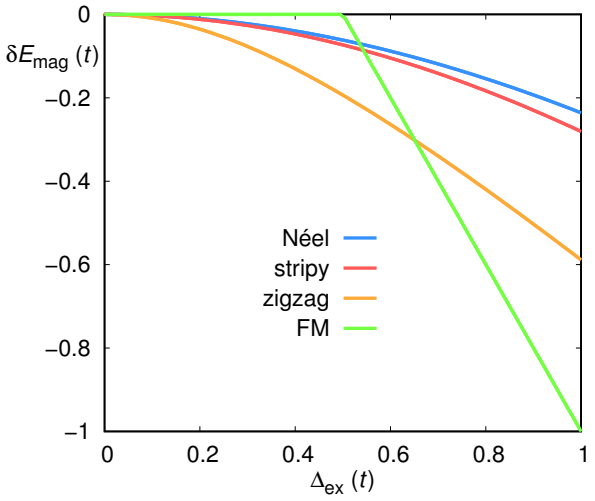

FIG. 7: One-electron DFT energy gain in the QMO model with respect to the non-magnetic energy, as a function of the exchange splitting, for various magnetic configurations.

degenerate. It is easy to understand why the ferromagnetic state is overstabilized in the DFT calculations: the Stoner energy in DFT includes the unphysical Hund's rule coupling of each orbital to itself.

Introducing the spin-orbit coupling in the DFT calculations, interestingly, makes the system somewhat closer to the above model. Even though the upper bands are now hybridized, they are well separated and thus are better described by the Hamiltonian of Eq. (3). Additionally, the zigzag phase, as opposed to the stripy one, retains the gap at the Fermi level, which gives it an additional energy advantage. As a result, the calculations with spin-orbit coupling firmly place the zigzag structure below the stripy one, although the ferromagnetic state is still competitive with the zigzag structure, for the reason discussed above [21]. Adding an atomic U makes the magnetic moments and gaps larger but does not change the energy hierarchy (we remind the reader that a physically meaningful accounting for a Hubbard U should be done for the QMOs, not the atomic orbitals).

To summarize, we have constructed a complete model of the electronic structure of a system of t_{2g} orbitals on a honeycomb lattice (of which Na_2IrO_3 is an example) in the case where the dominant metal-metal hopping is the n.n. hopping *via* oxygen and this hopping and the resulting band width is the largest energy scale in the system (which is the case in Na_2IrO_3). The model appears to be highly nontrivial and very remote from the popular Heisenberg-Kitaev model. The main factor defining the electronic structure is formation of quasi-molecular composite orbitals[22], akin to the textbook molecular orbitals of benzene or a SH_6 ring. In the first approximation, the QMOs on different hexagons are orthogonal, therefore the material forms already in non-relativistic calculations a system of narrow (~ 200 meV) subbands. The spin-orbit interaction is basically quenched for the lower two subbands, while for the upper two it leads to an additional interaction between the quasi-molecular composite orbitals, and emphasizes further the splitting of the t_{2g} band into four subbands. In the paramagnetic state, as well as in the antiferromagnetic zigzag state, only the uppermost band is empty, thus forming a band insulator. Correlation effects, while weak in terms of the ratio of the atomic U over the total t_{2g} band width, are moderately strong in terms of QMOs, thanks to the small band width of the molecular subbands. An analysis of the one-electron energy of the QMOs in the presence of an antiferromagnetic order reveals that, in agreement with the experiments, the so-called zigzag order is energetically favorable over the two competing antiferromagnetic orders, Néel and stripy, by a substantial margin. Our results open a completely new window on this intriguing compound and hopefully will lead to new theoretical and experimental research, now on the solid basis of a well-understood electronic structure. In particular, it will be instructive to address the superexchange between the QMO in the same way it is usually done for atomic orbitals; this is a subject for future work.

I.I.M. acknowledges many stimulating discussions with Radu Coldea and his group, and with Alexey Kolmogorov, and is particularly thankful to Radu Coldea for introducing him to the world of quasihexagonal iridates. H.O.J., R.V. and D.Kh. acknowledge support by the Deutsche Forschungsgemeinschaft through grants SFB/TR 49 and FOR 1346 (H.O.J. and R.V.) and SFB 608 and FOR 1346 (D.Kh.). H.O.J. acknowledges support by the Helmholtz Association via HA216/EMMI.

[1] Y. Singh and P. Gegenwart, Antiferromagnetic Mott insulating state in single crystals of the honeycomb lattice material Na_2IrO_3, Phys. Rev. B **82**, 064412 (2010).

[2] J. Chaloupka, G. Jackeli, and G. Khaliullin, Kitaev-Heisenberg Model on a Honeycomb Lattice: Possible Exotic Phases in Iridium Oxides A_2IrO_3, Phys. Rev. Lett. **105**, 027204 (2010).

[3] J. Reuther, R. Thomale, and S. Trebst, Finite-temperature phase diagram of the Heisenberg-Kitaev model, Phys. Rev. B **84**, 100406(R) (2011).

[4] G. Jackeli, and G. Khaliullin, Mott Insulators in the Strong Spin-Orbit Coupling Limit: From Heisenberg to a Quantum Compass and Kitaev Models, Phys. Rev. Lett. **102**, 017205 (2009).

[5] A. Shitade, H. Katsura, J. Kuneš, X.-L. Qi, S.-C. Zhang, and N. Nagaosa, Quantum Spin Hall Effect in a Transition Metal Oxide Na_2IrO_3, Phys. Rev. Lett. **102**, 256403 (2009).

[6] A. Kitaev, Anyons in an exactly solved model and beyond, Ann. Phys. (N.Y.) **321**, 2 (2006).

[7] Y. Singh, S. Manni, J. Reuther, T. Berlijn, R. Thomale, W. Ku, S. Trebst, and P. Gegenwart, Relevance of the

Heisenberg-Kitaev Model for the Honeycomb Lattice Iridates A_2IrO_3, Phys. Rev. Lett. **108**, 127203 (2012).

[8] In a competing paper[5], this ferromagnetic exchange was, on the contrary, entirely neglected, and an antiferromagnetic topological insulator was predicted.

[9] S. K. Choi, R. Coldea, A. N. Kolmogorov, T. Lancaster, I. I. Mazin, S. J. Blundell, P. G. Radaelli, Y. Singh, P. Gegenwart, K. R. Choi, S.-W. Cheong, P. J. Baker, C. Stock, and J. Taylor, Spin Waves and Revised Crystal Structure of Honeycomb Iridate Na_2IrO_3, Phys. Rev. Lett. **108**, 127204 (2012).

[10] F. Ye, S. Chi, H. Cao, B. C. Chakoumakos, J. A. Fernandez-Baca, R. Custelcean, T. Qi, O. B. Korneta, G. Cao, Direct evidence of a zigzag spin chain structure in the honeycomb lattice: A neutron and x-ray diffraction investigation on single crystal Na_2IrO_3, arXiv:1202.3995 (unpublished).

[11] S. V. Streltsov and D. I. Khomskii, Electronic structure and magnetic properties of pyroxenes $(Li,Na)TM(Si,Ge)_2O_6$: Low-dimensional magnets with 90° bonds, Phys. Rev. B **77**, 064405 (2008).

[12] We used for the calculations various full potential all electron codes, such as WIEN2k, ELK, and FPLO, and verified that the results agree reasonably well among different codes. Such comparison is particularly important because the codes implement the spin-orbit coupling in slightly different ways, employing usually unimportant, but in principle unequal approximations. In the *non-relativistic* calculations the core electrons were treated fully relativistically and the valence electrons non-relativistically (scalar relativistic approximation). In the *fully relativistic* calculations, *i.e.* with inclusion of spin-orbit coupling, all electrons were treated fully relativistically.

[13] M. S. Dresselhaus, G. Dresselhaus, and A. Jorio, *Group Theory: Application to the Physics of Condensed Matter,* Springer, 2008, Section 7.5.3. Note that exactly the same problem arises in calculating the electronic structure of the p_π levels in the actual benzene molecule, and is well known in quantum chemistry.

[14] One exception, which we cannot rationalize microscopically, is that two out of 6 different n.n. hoppings with $t_{dd\pi}$ symmetry appear comparable with t_2' ($\sim$ 70 meV) and 2.5 times larger than t_1. The other $t_{dd\pi}$ are much smaller.

[15] D. Pillay, M. D. Johannes, I. I. Mazin, O. K. Andersen, Origin of a_{1g} and e_g' orderings in Na_xCoO_2, Phys. Rev. B **78**, 012501 (2008).

[16] As DFT generally underestimates band gaps, for instance, Ge also comes out as a semimetal, such semimetallic DFT band structure is consistent with the experimentally observed semiconducting behavior.

[17] X. Liu, T. Berlijn, W.-G. Yin, W. Ku, A. Tsvelik, Y.-J. Kim, H. Gretarsson, Y. Singh, P. Gegenwart, and J. P. Hill, Long-range magnetic ordering in Na_2IrO_3, Phys. Rev. B **83**, 220403(R) (2011).

[18] R. Comin, G. Levy, B. Ludbrook, Z.-H. Zhu, C.N. Veenstra, J.A. Rosen, Y. Singh, P. Gegenwart, D. Stricker, J.N. Hancock, D. van der Marel, I.S. Elfimov, A. Damascelli, Na_2IrO_3 as a spin-orbit-assisted antiferromagnetic insulator with a 350 meV gap, arXiv:1204.4471 (unpublished).

[19] A. G. Petukhov, I. I. Mazin, L. Chioncel and A. I. Lichtenstein, Correlated metals and the LDA+U method, Phys. Rev. B **67**, 153106 (2003).

[20] O. Gunnarsson. Alkali-doped fullerides: narrow-band solids with unusual properties. World Scientific, 2004.

[21] We intentionally avoid strong quantitative statements about the ground state in the first principle calculations, for the following reasons: (1) the energy differences involved are of the order of a few meV per formula unit; the difference among different density functionals, as well as among particular implementations of the spin-orbit interaction, is also of that order, thus making definitive conclusions impossible; (2) given the small band width of the individual subbands, even a small U can make a difference relevant on the scale of a few meV, but no implementation of LDA+U on the level of QMOs, rather than atomic orbitals, is at present available; (3) Na_2IrO_3 being an itinerant magnet with possible magnetic frustration is bound to have contributions coming from quantum fluctuations. These contributions are not included in the DFT and may also contribute to the energy by a few meV. A detailed comparison of the magnetic energies obtained in different first principles methods (VASP, WIEN2k, ELK, and FPLO) will be published elswhere (P. Blaha, H.O. Jeschke, A. Kolmogorov, J.K. Dewhurst, I.I. Mazin, S. Sarma, R. Valentí *et al.*, to be published).

[22] We would like to note that the electronic structure of molecular crystals, where atoms can be partitioned into weakly coupled groups, has been considered before; what is unique about the present case is that each Ir atom participates in three different QMOs, and formation of QMOs does not lead to, nor follows from any atomic clusterization; hence the word "quasi".

Formation of molecular orbitals and suppression of spin-orbit coupling in Na_2IrO_3

I. I. Mazin,[1] H. O. Jeschke,[2] R. Valentí,[2] and D. I. Khomskii[3]

[1] *Code 6393, Naval Research Laboratory, Washington, DC 20375, USA*
[2] *Institut für Theoretische Physik, Goethe-Universität Frankfurt am Main, 60438 Frankfurt am Main, Germany*
[3] *II. Physikalisches Institut, Universität zu Köln, Zülpicher Strasse 77, 50937 Köln, Germany*

(Dated: May 16, 2012)

The electronic structure calculations for Na_2IrO_3 shown in this supplement were performed with the full potential local orbital (FPLO) code[1] using the generalized gradient approximation functional in its PBE form[2] and based on the C2/m structure as given in Ref. 3.

Fig. 1 shows the band structure of ferromagnetic Na_2IrO_3 without taking spin-orbit interaction into account. The high symmetry points used in Figure 1 and in all further band structures are $R = (1/2, 1/2, 1/2)$, $X = (1/2, 0, 0)$ and $M = (1/2, 1/2, 0)$, given in units of the reciprocal lattice vectors.

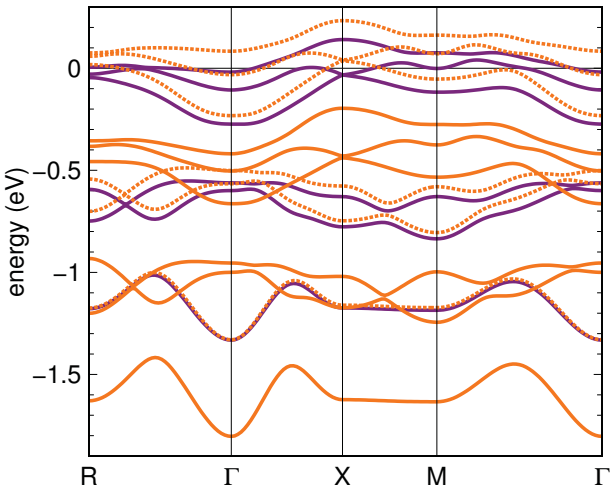

FIG. 1: Band structure of the ferromagnetic Na_2IrO_3 without including spin-orbit interaction. The two line types indicate the two polarizations. Purple lines show the parent nonmagnetic band structure. The Fermi levels in both cases were aligned at $E = 0$.

We use projective Wannier functions[4] to determine a tight binding (TB) representation for the Ir 5d bands. Figure 2 shows the DFT band structure together with the bands corresponding to the Wannier representation and the TB bands derived from this representation.

Figure 3 shows projective Wannier functions for the 5d orbitals of one Ir site. The Wannier functions exhibit the typical shape of the 5d functions at the Ir site. Besides, they show a clear asymmetry due to Na as well as tails on the O sites.

Figure 4 shows the band structure that results if we restrict the tight binding Hamiltonian to first neighbours

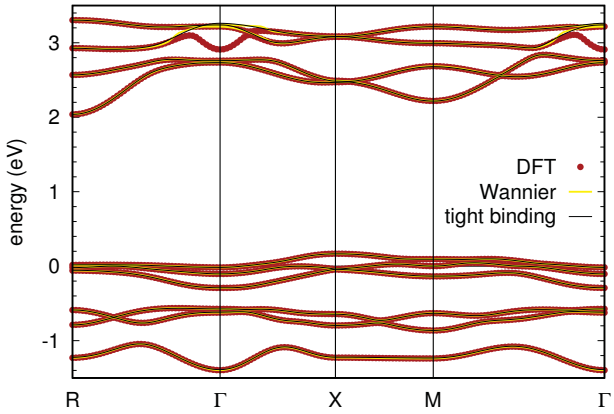

FIG. 2: Band structure of Na_2IrO_3 (red symbols) shown together with the Wannier bands (yellow) and the tight binding bands (blue).

(top left), up to second nearest neighbours (top right), up to third nearest neighbours (bottom left), and without restriction (bottom right).

In Figure 5 we show the tight binding band structures that are restricted to tight binding parameters which contribute to the quasi-molecular orbitals. The four panels represent onsite terms only (onsite energy and trigonal distortion, top left), up to first nearest neighbours (top right), up to second nearest neighbours (bottom left) and up to third nearest neighbours (bottom right). Note that the small dispersion that arises for nearest neighbours is due to deviations from the perfect octahedral environment of iridium. This is most likely also the reason why for second nearest neighbours the ideal 1-2-2-1 degeneracy is lost near the Fermi level.

[1] K. Koepernik and H. Eschrig, Phys. Rev. B **59**. 1743 (1999); http://www.FPLO.de
[2] J. P. Perdew, K. Burke and M. Ernzerhof, Phys. Rev. Lett. **77** 3865 (1996).
[3] S. K. Choi, R. Coldea, A. N. Kolmogorov, T. Lancaster, I. I. Mazin, S. J. Blundell, P. G. Radaelli, Yogesh Singh,

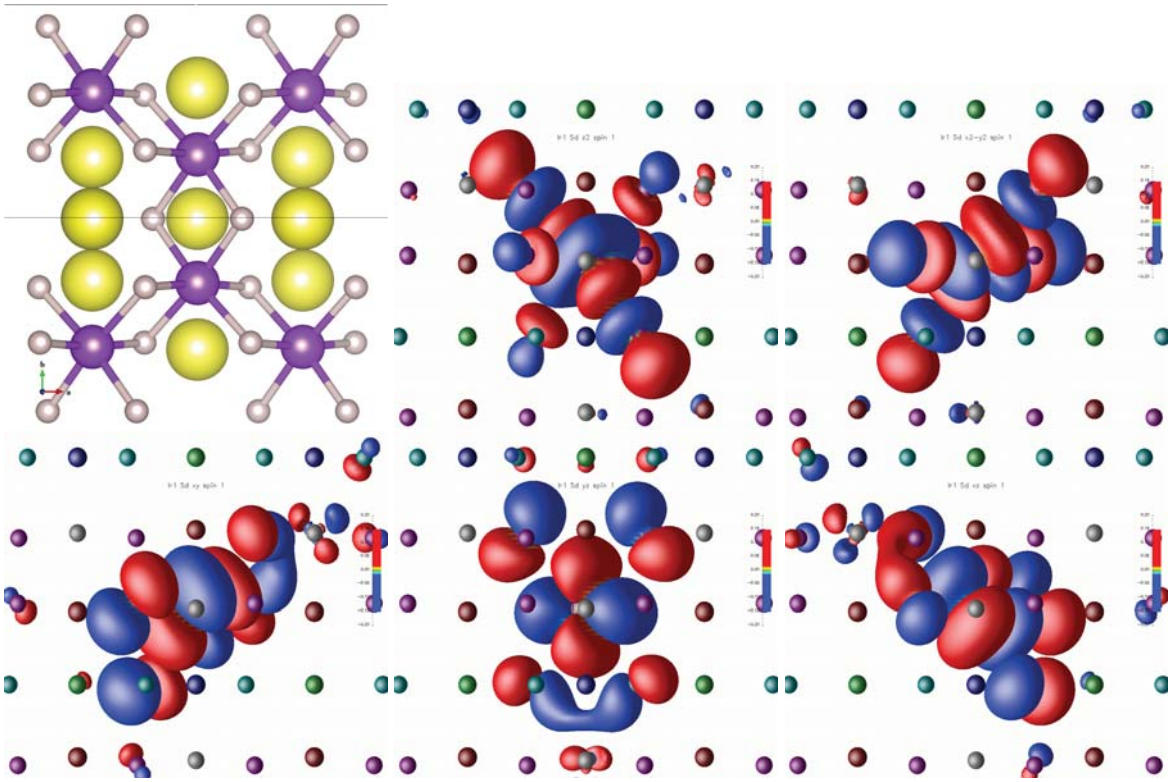

FIG. 3: Projective Wannier functions for five of the ten Ir 5*d* bands, together with a structure showing the perspective.

P. Gegenwart, K. R. Choi, S.-W. Cheong, P. J. Baker, C. (2009).
Stock, J. Taylor, Phys. Rev. Lett. **108**, 127204 (2012).
[4] H. Eschrig and K. Koepernik, Phys. Rev. B **80**, 104503

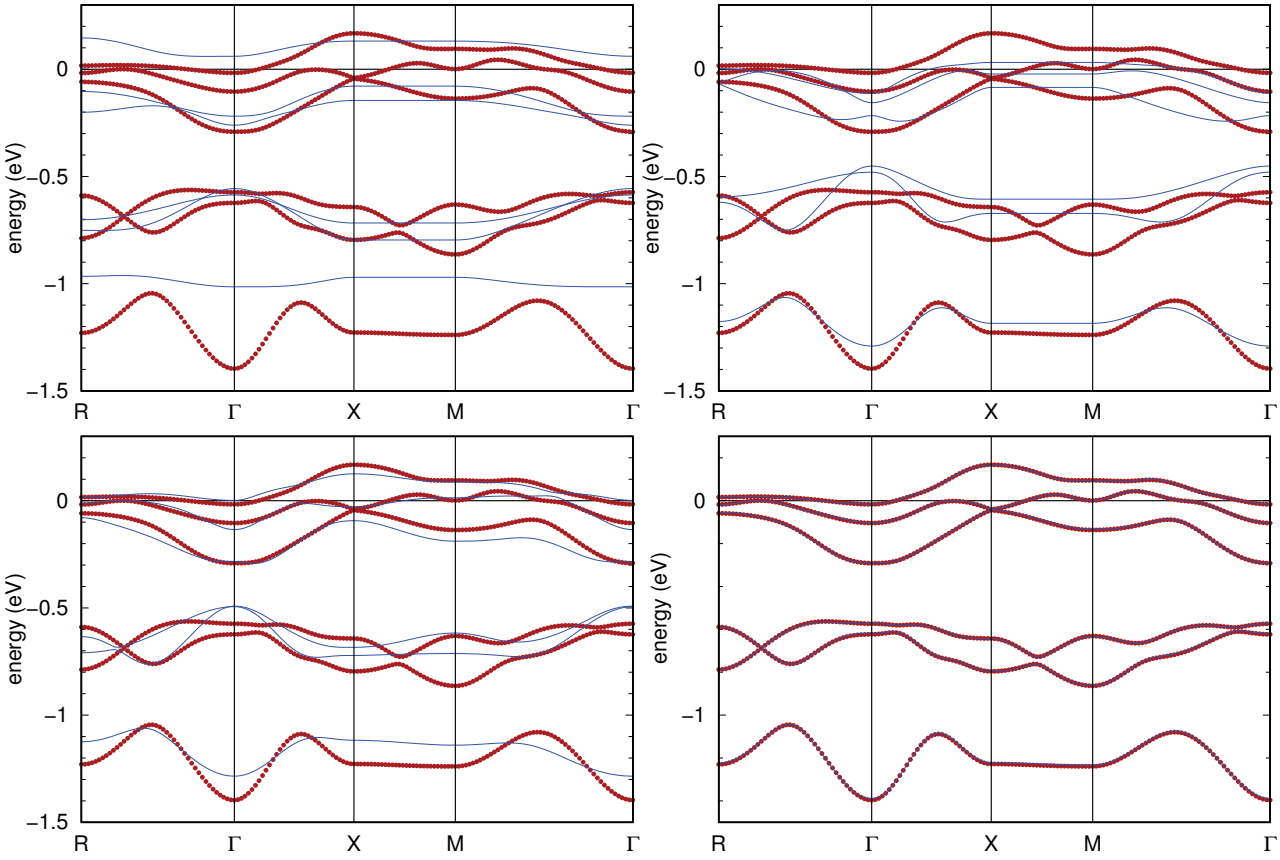

FIG. 4: Band structure of Na_2IrO_3 (red symbols) shown together with the tight binding models that include only nearest neigbours (top left), up to next nearest neighbours (top right), up to third nearest neighbours (bottom left) and neighbours up to 16 Å (bottom right).

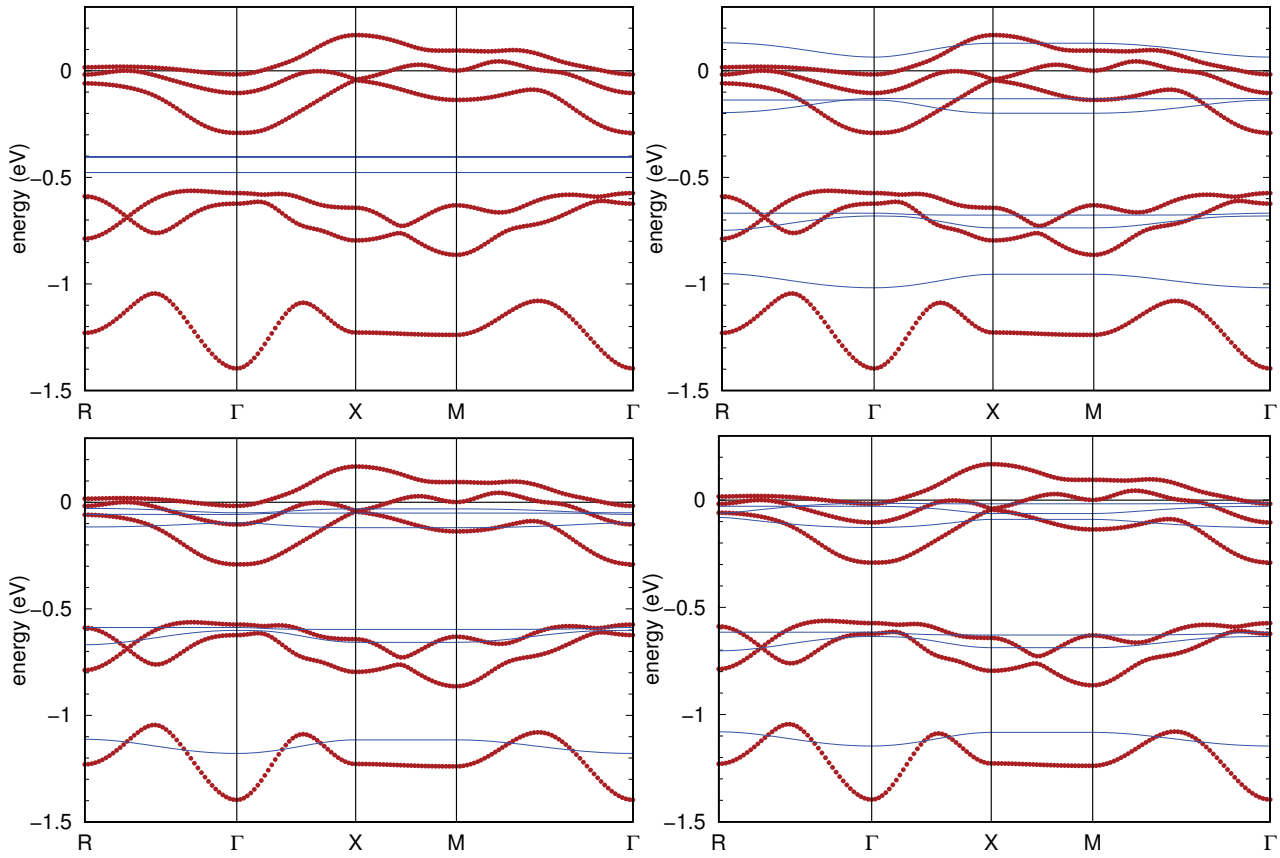

FIG. 5: Band structure of Na_2IrO_3 (red symbols) shown together with the tight binding models that involve only parameters compatible with the quasi-molecular orbitals. Only on-site parameters (top left), up to nearest neighbours (top right), up to second nearest neighbours (bottom left) and up to third nearest neighbours (bottom right).